CSID Journal of Infrastructure Development

Volume 2 | Issue 2 Article 10

12-31-2019

Finite Element Modelling and Parametric Studies of Semi-Closed Thin-Walled Steel Polygonal Columns For The Application on Steel Lattice Towers

Bona Ryan
Department of Civil, Environmental and Natural Resources Engineering, Luleå University of Technology, University Campus Porsön, Luleå, SE-97187 Luleå, Sweden, bona8787@gmail.com

Efthymios Koltsakis
Department of Civil, Environmental and Natural Resources Engineering, Luleå University of Technology, University Campus Porsön, Luleå, SE-97187 Luleå, Sweden, efthymios.koltsakis@ltu.se

Panagiotis Manoleas
Department of Civil, Environmental and Natural Resources Engineering, Luleå University of Technology, University Campus Porsön, Luleå, SE-97187 Luleå, Sweden, panagiotis.manoleas@ltu.se

Follow this and additional works at: https://scholarhub.ui.ac.id/jid

Recommended Citation
Ryan, B., Koltsakis, E., & Manoleas, P. (2019). Finite Element Modelling and Parametric Studies of Semi-Closed Thin-Walled Steel Polygonal Columns For The Application on Steel Lattice Towers. *CSID Journal of Infrastructure Development, 2*(2), 204-214. https://doi.org/10.32783/csid-jid.v2i2.65

This Article is brought to you for free and open access by UI Scholars Hub. It has been accepted for inclusion in CSID Journal of Infrastructure Development by an authorized editor of UI Scholars Hub.

Finite Element Modelling and Parametric Studies of Semi-Closed Thin-Walled Steel Polygonal Columns For The Application on Steel Lattice Towers

Cover Page Footnote

-

This article is available in CSID Journal of Infrastructure Development: https://scholarhub.ui.ac.id/jid/vol2/iss2/10

CSID Journal of Infrastructure Development (2)2: 204-214
ISSN 2407-4438 © CSID-JID 2019

FINITE ELEMENT MODELLING AND PARAMETRIC STUDIES OF SEMI-CLOSED THIN-WALLED STEEL POLYGONAL COLUMNS FOR THE APPLICATION ON STEEL LATTICE TOWERS

Bona Ryan[1*], Efthymios Koltsakis[2*], Panagiotis Manoleas[3*]

[1, 2, 3]*Department of Civil, Environmental and Natural Resources Engineering, Luleå University of Technology, University Campus Porsön, Luleå, SE-97187 Luleå, Sweden*

(Received: September 2019 / Revised: December 2019 / Accepted: December 2019)

ABSTRACT

The trend of structural engineering in the recent years is toward the use of lighter and more economical structural elements. In steel construction, peculiarly, main structural member composed by thin-walled elements are being explored by researchers due to their potential to offer better solution with economical features. However, the use of slender profiles and a complex cross sections shape lead to requirements to study instability phenomenon in a form of local, distortional, flexural, torsional and coupled instability. Such complex structural behaviour is inevitably accompanied by demand to improve calculation methods and design provisions. In this context an innovative solution of structural element composed of thin-walled plates is proposed for the application on lattice support structure of wind turbine. A semi-closed section is made by assembling series of folded plates into polygonal profiles with mechanical fasteners, loaded in compression and bending moment which occurs as the effect of forces acting on the connection. The expected structural behaviour of the column is a mixture between the open and closed cross-section. These cases will be investigated through numerical analysis and parametric studies of the proposed profiles for the investigation of buckling behaviour and ultimate resistance, respectively.

Keywords: Buckling; Finite element analysis; Semi-closed polygonal section; Thin-walled element

1. INTRODUCTION

Thin-walled cold-formed structural members are becoming more popular and have a growing importance. One of the reasons is the versatile nature which allows for the forming of almost any section geometry which can be produced at low-cost by cold forming and rolling from thin steel sheets. Other advantages such as high strength-to-weight ratio, reduced labour costs and fast erection due to the light weight of cold-formed members have been promoting its extensive applicability. Cold-formed steel sections are usually thinner than hot–rolled sections and can be subject to different modes of failure and deformation and therefore extensive testing is required to provide a guideline for the design of cold-formed thin-walled structural members (Yu, LaBoube, & Chen, 2019).

*Corresponding author's email:
[1]bona-rya@ltu.se, bona8787@gmail.com, orcid.org/0000-0003-3385-6860
[2]efthymios.koltsakis@ltu.se, orcid.org/0000-0001-6150-7241
[3]panagiotis.manoleas@ltu.se, orcid.org/0000-0002-9338-671x

Thin-walled cold-formed profiles are usually made from cold rolled coils and folded in the second step. In this way, only open profiles can be produced. The predominant problem of this individual plate open cross-section is the excessive torsional effect, which is unfavourable for compressive members. This means that the resistance to global buckling frequently is governed by torsional or torsional-flexural buckling with a relatively low resistance compared to flexural buckling. A better response is possible with closed cross sections, but such profiles could not be produced by the folding. The solution is to make semi-closed section by assembling them into polygonal profiles with mechanical fasteners, as presented in this research. It is here called a semi-closed cross-section because it is not continuously and rigidly connected.

Figure 1 shows possible polygonal profiles for compression chords and diagonals in a lattice. The gusset plates required for the connections are inserted into the polygonal profile and secured with pretension bolts.

Figure 1 Illustration of individual plate and the proposed semi-closed polygonal cross section for chords and diagonals

2. STATE OF THE ART

In the current design of steel towers for onshore wind turbines the most common type of tower is cylindrical tubular tower. Some challenging limitations regarding tower height and erection process attributed to this type of structures including transportation restriction for maximum shell diameter of 4 - 4.5*m*, fatigue endurance due to transversal and longitudinal welding, connection problems with thick flanges, expensive rolling process, and lifting technology that limit the height of current installed tower to be 80 - 100*m*. Lattice or truss support structure then proposed to deal with such problems, however the steel CHS section as common cross section for this type of structure has complication in welding connection and member thickness. All these issues will eventually affect the cost effectiveness of tower component in the overall building cost. Many researches have been looking for different solutions to these problems. Three projects which have been dealing with these questions are from Milan Veljkovic et al. (2012), M Veljkovic et al. (2014), and the most recent from European Comission (2016). New challenging load conditions and new type of support structures for wind energy converter which foster new structural concepts and high performance material became the focus of those researches. As part of these projects, Heistermann (2011) proved a new solution with friction connections to replace the traditional in flange connection, and then Garzon (2013) conducted comprehensive study of polygonal tubular towers made of folded plates. However, the research of lattice towers made of semi-closed polygonal columns has not been conducted yet, thus this type of structural member is adopted in this research. Globally, the work is intended to promote competitiveness of semi-closed polygonal cross section for truss structure application.

Unlike heavy hot-rolled steel sections, cold-formed thin-walled sections tend to buckle locally at stress levels lower than the yield strength of the material, characterised by the relatively short wavelength buckling of individual plate element. However, these members do not fail at these stress levels and continue to carry further loads, which is called post-buckling behaviour. In thin-walled cold-formed steel structures, elastic bucking and load deformation response are closely related (Teng & Rotter, 2006). There are different possible buckling modes: Local, Distortional, Euler (Flexural), Torsional-Flexural of column or Lateral-Torsional of beam (B. Schafer & Peköz, 1999). Overall column strength is greatly dependent on the interaction effect of local and overall column buckling. The curves shown in Figure 2 have been obtained using elastic Finite Strip (FS) method, analysing and describing the change of buckling strength versus buckle half-wavelength.

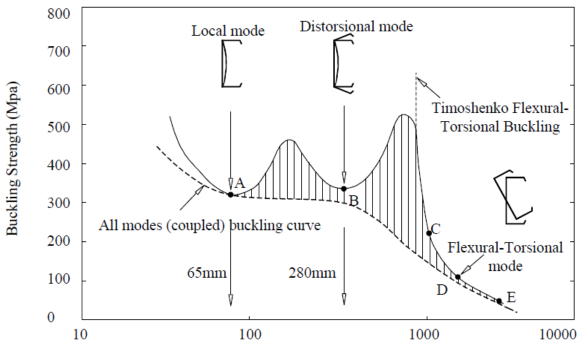

Figure 2 Buckling strength versus half-wavelength for a lipped channel in compression
Sources: (Hancock, 1997)

In general, the buckling mode is influenced by cross-section geometry, end conditions, loading and material. Also, introducing openings and imperfections to structures has a significant effect on the critical buckling load and the buckling mode (B. W. Schafer, 2006). The dashed line in Figure 2, qualitatively shows the pattern of all modes or coupled mode. The effect of interaction between sectional and global buckling modes results in increasing sensitivity to imperfections, leading to the erosion of the theoretical buckling strength (Dubina, 2014).

The design procedure stated in Eurocode EN 1993-1-3 (European committee for standardization, 2006) applies limited only for the cross sectional types mentioned in the design code, which are open cross sections, and does not cover specific built-up member. Therefore, one of the objectives of this research is to rule out structural characteristics of the proposed section for design recommendation.

3. METHODOLOGY

In order to gain a deeper understanding and formulate hypotheses for the structural behaviour of semi-closed thin-walled steel columns with polygonal section, a comprehensive numerical analysis and parametric studies was carried out by means of FE modelling in ABAQUS package. Both processes were created through scripting using MATLAB and Python.

First, the profiles geometrical database of the sections was generated by using MATLAB code. This database was then exported to Python via pickle file. Then the automation was performed in Python environment that will be fed to ABAQUS. The modelling process in Python was carried out through back and forth process between ABAQUS/CAE and Python to build the final working models and eventually used as an input file for ABAQUS. This input file of all models was then run simultaneously in batch mode of ABAQUS platform.

The analysis requires three steps: (i) pre-processing to build up the FE model and generate the input file, (ii) job-running, and (iii) post-processing to extract the results. Basically, the ABAQUS scripting is a Python-based application programming interface (API) to ABAQUS. Thus, it is an advantage to utilize Python for FE modelling and analyses in ABAQUS.

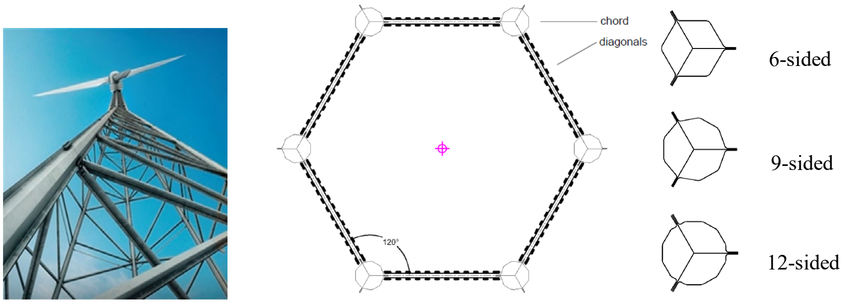

Figure 3 Base view of the studied tower

The chord is a built-up member composed of folded plates and gusset plates. The close-up picture of the member is shown in Figure 4. Assembly of the member is performed by bolting them along the lips of the folded plate at a specified spacing. As for the connection between chord and diagonals, gusset plates coming out from the core of the chord provide the joint.

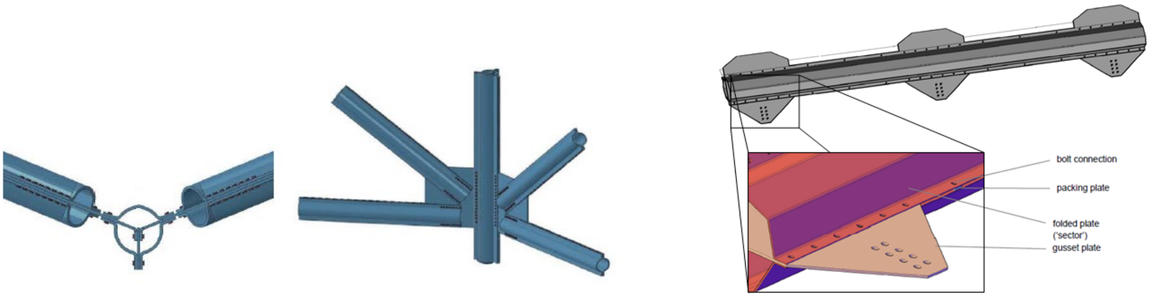

(a) (b)

Figure 4 (a) Illustration of chord-to-diagonals bolted connection;
(b) Extruded view of the studied column

The modelling and design process of this research is fully described in Ryan (2017) and here only a summary will be given. The material property given by EC3 for cold-formed profile and used in the normal production is S355, which elastic properties are summarized in Table 1.

Table 1 Steel property used

Type of steel	Grade	F_{yb} [N/mm^2]	F_u [N/mm^2]
Non-alloy structural steel	S 355	355	510

The plastic characteristic of steel was taken from relationship between yield stress and plastic strain defined based on uniaxial coupon test data. The testing machine measured total strain and reaction value of each specimen from elastic range until failure. It is worth noting that the true stress-strain data was used as input into ABAQUS as a series of data points.

Ranges of values for each parameter used in the parametric study are tabulated in the Table 2. In order to complete the FE modelling and analyses optimally in the predefined time, the number of input variables used in this parametric study were reduced, so that only some input variables of the parameter were taken from the database.

Based on Table 2 above there are five parameters accounted in this study, namely *n*, *d*, *slend, len,* and *b_ratio* which will determine the naming of numerical model. *l_ratio* and *t_ratio* are functions based on the value of parameter. Parameter of bolt density (*b_ratio*) and length (*len*) are to be significant in the buckling behaviour of the member since they affect the buckling half-wave length of the member which in turn becomes decisive parameters for the buckling and interaction buckling failure mode.

Table 2 Ranges of parameter values

Parameter	Description	Function	Value(s)	Number of model for each profile	Total number of models acc.
n	number of corners	[6, 9, 12]	6	3	18
d	diameter of chord	[300:200:900]	500, 700, 900	3	
slend	profile slenderness	d/(ε².t) linspace(70,150,10)	90, 110	2	
fy	yield strength	355	355	1	
rcoef	bending radius to thickness ratio	6	6	1	
nbend	number of points along the bend	5	5	1	
l_ratio	lip length to diameter ratio	0.1	0.1	1	
t_ratio	gusset to sector thickness ratio	1.2	1.2	1	
len	length of chord	$\bar{\lambda} = \left(\frac{A.f_y.l^2}{\pi^2 EI_y}\right)^{0.5}$	0.65, 1.0, 1.25	3	
b_ratio	bolt density	s/d	3.0, 4.0, 5.0	3	54
N	Axial force	-	N	1	54
NM	Axial force-bending moment	-	0.05M, 0.1M, 0.15M	3	216

The length of chord is calculated by keeping the non-dimensional slenderness, $\bar{\boldsymbol{\lambda}}$, to certain values, which are 0.65, 1.0, and 1.25. These values were chosen to make sure the member will not either be too slender or too stocky. The calculation requires cross-section properties: area of closed cross-section, *A*, and moment of inertia, *I*, and this was carried out in MATLAB script and stored in meta file which then used in the Python script.

Five primary parameters which have varied values: *n*, *d*, *slend*, *len*, and *b* determine the naming of numerical model. In order to make easy identification, it was decided to name the models with numbers, as follows.

i - ***j*** - ***k*** - ***l*** - ***b***

i …number of corners (n)
j …diameter (d)
k …slenderness (slend)
l …length (len)
b …bolt spacing (b_ratio)

The variable number for naming and the corresponding value is shown in the table below.

	i			**j**				**k**		**l**			**b**		
var. ID	1	2	3	1	2	3	4	3	5	1	2	3	1	2	3
values	6	9	12	300	500	700	900	90	110	0.65	1.0	1.25	3	4	5

4. RESULTS AND DISCUSSION

4.1. FE Elastic Buckling and Non-linear Analysis

4.1.1 Verification of Elastic Buckling Analysis

A geometrical and material non-linear analysis with imperfection (GMNIA) was used in this work. However, determination of an accurate elastic buckling load and mode shape is important to the existing design method (Moen, 2008). The correlation between the elastic buckling and ultimate resistance of cold-formed members provides the basis for the design strength.

Buckling mode shape of the models with the lowest non-dimensional global slenderness ($\bar{\lambda}$), i.e. 0.65 are characterized by distortional buckling of the sector plate in between the lip's bolt connection, whereas higher non-dimensional slenderness, i.e. 1.0 and 1.25 were dominated by flexural buckling and interaction flexural-distortional buckling. This phenomenon occurs since $\bar{\lambda}$ correlated with length of the member or half-wave length of the buckling.

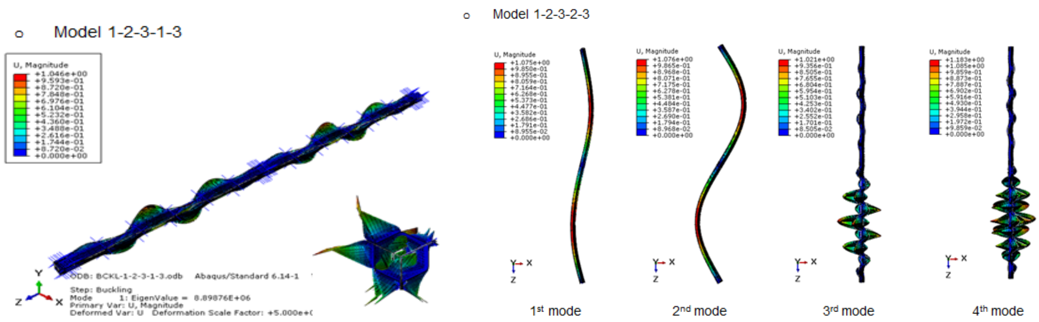

Figure 5 First buckling of Model 1-2-3-1-3

In this analysis, buckling analyses were performed for four eigenvalues and mode shapes for all models. It was shown that from the other buckling mode shapes, the deformations of the models were changing and unsymmetrical. It proves that in some cases, choosing a suitable buckling mode shape is complicated. It will influence on the cost of performing the analysis and accuracy of the results. Therefore, in this study the imperfection took the first until the fourth mode shapes in order to make it more realistic.

Table 3 First critical load according to elastic buckling analysis

(a) d-parameter=500

Model ID	Dia. d [mm]	Thick. t [mm]	Slend. λ [-]	Length l [mm]	bolt spacing s/d [-]	Elastic theory (Euler buckling) N_{crit} [kN]	Numerical Analysis (FEM) N_{crit} [kN]	Buckling mode
1 2 3 1 3					3	11095	8899	dist.
1 2 3 1 4			0.65	18098	4	11095	6645	dist.
1 2 3 1 5					5	11095	5357	dist.
1 2 3 2 3					3	4972	5099	flex.
1 2 3 2 4		9	1	27035	4	4972	5021	flex.
1 2 3 2 5					5	4972	4889	dist.
1 2 3 3 3					3	3254	3382	flex.
1 2 3 3 4			1.25	33419	4	3254	3350	flex.
1 2 3 3 5	500				5	3254	3308	flex.
1 2 5 1 3					3	8692	5995	dist.
1 2 5 1 4			0.65	18106	4	8692	4413	dist.
1 2 5 1 5					5	8692	3540	dist.
1 2 5 2 3					3	3895	4001	flex.
1 2 5 2 4		7	1	27048	4	3895	3936	flex.
1 2 5 2 5					5	3895	3182	dist.
1 2 5 3 3					3	2549	2654	flex.
1 2 5 3 4			1.25	33435	4	2549	2628	flex.
1 2 5 3 5					5	2549	2594	flex.

(b) d-parameter=700

Model ID	Dia. d [mm]	Thick. t [mm]	Slend. λ [-]	Length l [mm]	bolt spacing s/d [-]	Elastic theory (Euler buckling) N_{crit} [kN]	Numerical Analysis (FEM) N_{crit} [kN]	Buckling mode
1 3 3 1 3					3	20741	15768	dist.
1 3 3 1 4			0.65	25339	4	20741	11605	dist.
1 3 3 1 5					5	20741	9277	dist.
1 3 3 2 3					3	9295	9487	flex.
1 3 3 2 4		12	1	37852	4	9295	9333	flex.
1 3 3 2 5					5	9295	8383	dist.
1 3 3 3 3					3	6083	6300	flex.
1 3 3 3 4			1.25	46790	4	6083	6239	flex.
1 3 3 3 5	700				5	6083	6157	flex.
1 3 5 1 3					3	17374	11900	dist.
1 3 5 1 4			0.65	25347	4	17374	8683	dist.
1 3 5 1 5					5	17374	6907	dist.
1 3 5 2 3					3	7785	7933	flex.
1 3 5 2 4		10	1	37865	4	7785	7797	flex.
1 3 5 2 5					5	7785	6169	dist.
1 3 5 3 3					3	5095	5271	flex.
1 3 5 3 4			1.25	46806	4	5095	5218	flex.
1 3 5 3 5					5	5095	5147	flex.

Results of elastic buckling analysis for all models are presented in Table 3. It can be seen from the table that the theoretical or Euler elastic buckling calculations based on EN1993-1-1 have a disagreement on the FEM analysis critical load for models with distortional-controlled buckling. In this case, the Euler critical loads are much higher than results from FEM analysis since the Euler buckling formulae consider the member as a whole perfect column and for flexural case only, without taking into account local or distortional buckling and interaction between them. In other hand, FEM considers the real geometrical conditions, thus the effect of non-fully rigid connected plates to the buckling behaviour was taken into account.

4.1.2 Verification of Non-linear Analysis

The non-linear FE analysis using Riks solver was carried out for analyses of unstable, materially and geometrically nonlinear with imperfections considered. FE models uses four-node general-purpose shell element with finite membrane strains, elastic-plastic material with strain hardening, and imperfections based on Simulia (2007) documentation.

From the result in Table 4, it can be seen that the failure modes of the models are dominated by distortional failure with the remaining models show interaction distortional-flexural failure. The difference of this result to the elastic buckling analysis can be clearly noticed, where there is no independent global flexural failure mode in non-linear analysis. This affirms the significant influence of material and geometrical non-linearity and imperfections on the ultimate resistance of the studied models.

Table 4 Ultimate loads and corresponding displacement from FE non-linear analysis

(a) d-parameter=500

Model ID	Dia. [mm]	Thick. [mm]	Slend. [-]	Length [mm]	bolt spacing [-]	Max. load P_u [kN]	Shortening disp [mm]	Normalized resistance P_u/P_{yg} [-]	Failure mode
1 2 3 1 3					3	5625.7	29.13	1.00	dist.
1 2 3 1 4			0.65	18098	4	4982.5	26.03	0.89	dist.
1 2 3 1 5					5	4531.8	24.75	0.81	dist.
1 2 3 2 3					3	4865.7	37.93	0.87	dist.
1 2 3 2 4		9	1	27035	4	4555.0	35.44	0.82	dist.
1 2 3 2 5					5	4126.2	32.17	0.74	dist.
1 2 3 3 3					3	3335.7	34.09	0.60	dist-flex
1 2 3 3 4			1.25	33419	4	3269.5	33.10	0.59	dist-flex
1 2 3 3 5	500				5	3176.2	31.49	0.57	dist-flex
1 2 5 1 3					3	4132.5	27.34	0.95	dist.
1 2 5 1 4			0.65	18106	4	3576.7	24.21	0.82	dist.
1 2 5 1 5					5	3161.9	23.20	0.72	dist.
1 2 5 2 3					3	3665.2	36.35	0.84	dist.
1 2 5 2 4		7	1	27048	4	3241.9	32.20	0.74	dist.
1 2 5 2 5					5	2840.9	28.59	0.65	dist.
1 2 5 3 3					3	2606.7	33.78	0.60	dist-flex
1 2 5 3 4			1.25	33435	4	2496.8	31.14	0.57	dist-flex
1 2 5 3 5					5	2405.3	30.03	0.55	dist-flex

(b) d-parameter=700

Model ID	Dia. [mm]	Thick. [mm]	Slend. [-]	Length [mm]	bolt spacing [-]	Max. load P_u [kN]	Shortening disp [mm]	Normalized resistance P_u/P_{yg} [-]	Failure mode
1 3 3 1 3					3	10583.1	41.10	1.00	dist.
1 3 3 1 4			0.65	25339	4	9053.7	35.59	0.87	dist.
1 3 3 1 5					5	8140.8	33.86	0.78	dist.
1 3 3 2 3					3	8974.8	52.52	0.86	dist.
1 3 3 2 4		12	1	37852	4	8128.1	47.34	0.78	dist.
1 3 3 2 5					5	7400.3	43.45	0.71	dist.
1 3 3 3 3					3	6192.9	47.06	0.59	dist-flex
1 3 3 3 4			1.25	46790	4	6020.5	45.09	0.58	dist-flex
1 3 3 3 5	700				5	5901.9	43.72	0.57	dist-flex
1 3 5 1 3					3	8309.6	38.52	0.95	dist.
1 3 5 1 4			0.65	25347	4	7358.9	34.13	0.84	dist.
1 3 5 1 5					5	6417.5	32.86	0.74	dist.
1 3 5 2 3					3	7105.3	49.55	0.81	dist.
1 3 5 2 4		10	1	37865	4	6373.9	44.55	0.73	dist.
1 3 5 2 5					5	5661.1	40.01	0.65	dist.
1 3 5 3 3					3	5177.7	47.83	0.59	dist-flex
1 3 5 3 4			1.25	46806	4	4985.4	44.02	0.57	dist-flex
1 3 5 3 5					5	4683.0	40.90	0.54	dist-flex

The results of the parametric studies of all column models are presented in Figure 6 in the form of normalized resistance ($P_{u\text{-}FEM}/P_{yg}$) based on fully effective cross-section resistance (P_{yg}) versus local slenderness $\lambda_{cr\text{-}FEM} = (P_{yg}/P_{cr\text{-}FEM})^{0.5}$ based on P_{yg} and the critical buckling load by the FEM analysis. It is important to note that the failure mode of all models in this non-linear study is distortional type, while some of the first critical buckling loads by FEM discussed in previous section were the flexural type. Therefore, it is needed to obtain distortional buckling loads for those models in order to have proper local slenderness, according to the actual failure mode. This is performed by looking at other buckling modes which give distortional type of buckling in ABAQUS. Then, these critical buckling loads were taken for constructing the graph. Figure 6 also shows the EN1993-1-3 resistance curve for distortional buckling mode, and other codes for different corresponding buckling modes.

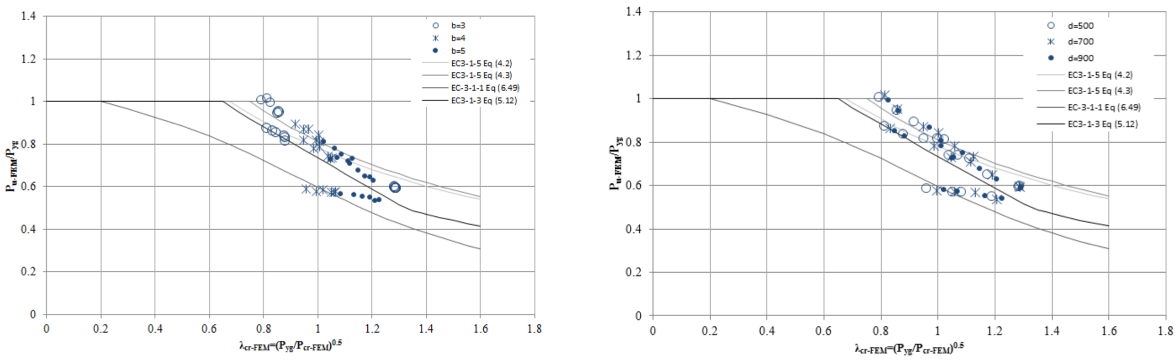

(a) grouped in bolt spacing (b) grouped in profile diameter

Figure 6 Parametric study results of the studied columns (normalized resistance based on P_{yg} vs. slenderness based on P_{yg} and FEM critical buckling loads)

From the graph it is worth noted that there are two obvious scatters of data points when slenderness $0.9 < \lambda_{cr\text{-}FEM} < 1.2$. The higher scatter group corresponds to those columns which failed in a pure distortional mode, while the lower scatter corresponds to those columns failed in distortional-flexural interaction. This means although the vast majority of the failure modes from the FEM are distortional modes, an interaction distortional-flexural failure did occur for models with high global slenderness, $\bar{\lambda} = 1.25$, in which give lower strength than the distortional modes. Figure 6 shows that in case of distortional failure, a full proportion of the numerical ultimate resistance were slightly underestimated by the design code, which means that EN1993-1-3 corresponds to the FEM analysis results and gives safe but less conservative prediction. It can be said that the EN1993-1-3 curve almost forms the lower bound of the numerical ultimate resistance for the studied models.

A small scatters of data points which appeared below the EN1993-1-3 strength curve in the graph are all models with global slenderness $\bar{\lambda}$ = 1.25, and a safe estimates of strength cannot be provided by EN1993-1-3 since it is an interaction modes. Very unsafe predictions were provided by the EN1993-1-3 curve for those models. These data points fell on local slenderness, i.e. $\lambda_{cr\text{-}FEM} \geq 0.9$ for models with bolt spacing ratio, $b = 4$ and larger slenderness $\lambda_{cr\text{-}FEM} \geq 1.0$ for models with $b = 5$. The flexural slenderness which was significantly high and larger than the distortional slenderness may induce the flexural deformation interacted with the distortional mode. It is suggested by this parametric study that the EN1993-1-3 curve provides safe (or almost safe) predictions if the columns fail in a pure distortional mode, whereas give unsafe prediction if the columns fail in interaction mode, D-F interaction in this case.

By travelling from the highest to the lowest $P_{u\text{-}FEM}/P_{yg}$ values, the scatter of data points corresponds to the increase of bolt spacing ratio b-parameter. This shows that with the increase of bolt spacing, being from $b = 3$ to $b = 4$ and $b = 5$, the ultimate resistance tends to decrease.

This graph shows that the non-dimensional slenderness and bolt spacing are the most influencing parameter which characteristics resulted in significantly deviated ultimate resistance. Likewise, the diameter d-parameter and thickness t-parameter give unfavourable effect on the ultimate resistance when it increases, however this influence is not significant and considerably lower than those caused by slenderness and bolt spacing.

From this analysis it can be noted that for the studied columns, distortional failures have lower post-buckling capacity than the other mode, i.e. local buckling. Furthermore, distortional buckling may control the failure mechanism even when the elastic distortional buckling stress (f_{crd}) is higher than the elastic flexural buckling stress (f_{crf}).

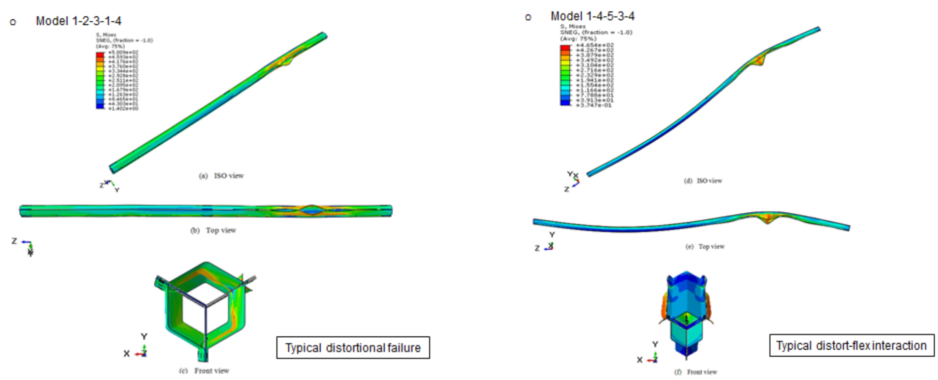

(a) (b)

Figure 7 Failure mode of a RIKS model failing (a) by distortional mode and (b) by distortional-flexural interaction mode

As a sample for visualization of failure mode, Figure 7(a) shows a typical distortional buckling mode at the ultimate load of model 1-2-5-1-3. The colour contours represent the magnitudes of von Misses stress. The failure is characterized by buckling of the lips outward, while no significant rotation along its weak axis experienced by the entire column. This type of buckling is also known as “stiffener flexural buckling” or “local-torsional buckling”. Lips as connection between plates in this type of sections can be considered as the stiffener. Distortional buckling exists at intermediate longitudinal half sine waves (half-wavelength), between short local buckling half-wavelength and long flexural or flexural-torsional buckling half-wavelength. In this case, the half-wavelength is the bolt spacing distance (s).

Meanwhile, Figure 7(b) shows the failure mode by interaction between distortional and flexural buckling for models with $\bar{\lambda}$ = 1.25. The failure mode is characterized by buckling of the lips outward and at the same time, large rotation of the entire member.

Moreover, this parametric study is expected to rule out the limit of normalized resistance for the expected failure mode, in this case distortional buckling, based on slenderness of the member. From graph in Figure 6, it can be suggested that the expression (Eq. 5.12) in EN1993-1-3 (CEN, 2009) for reduction factor due to distortional buckling may be adopted for the semi-closed polygonal type of cross-section undergoes pure distortional buckling mode used in this parametric study, with provision of global slenderness, $\bar{\lambda} < 1.25$. The EN1993-1-3 became the lower bound for the results of numerical ultimate strength.

$$\chi_d = 1.0 \qquad \text{if} \qquad \bar{\lambda}_d < 0.65;\ \bar{\lambda} < 1.25 \tag{1}$$

$$\chi_d = 1.47 - 0.723\bar{\lambda}_d \qquad \text{if} \qquad 0.65 < \bar{\lambda}_d < 1.38;\ \bar{\lambda} < 1.25 \tag{2}$$

$$\chi_d = \frac{0.66}{\bar{\lambda}_d} \qquad \text{if} \qquad \bar{\lambda}_d \geq 1.38;\ \bar{\lambda} < 1.25 \tag{3}$$

Meanwhile, a distortional-flexural interaction would be found in models with global slenderness $\bar{\lambda} = 1.25$. Therefore, by excluding the cluster data points of pure distortional mode, a linear regression was developed to get the expression of ultimate resistance as shown in Eq. 4.

$$\chi_{d-f} = 0.7576 - 0.1751\bar{\lambda}_d \quad \text{if} \quad 0.9 < \bar{\lambda}_d < 1.25;\ \bar{\lambda} \geq 1.25 \tag{4}$$

4.2. Analytical analysis according to the standard rules EN1993-1-3

In this section, the results from numerical analysis of the models used in parametric studies were compared and verified to the analytical calculations according to EN1993-1-3 *General rules for cold-formed members and sheeting*. Table 5 shows the result of analytical calculation according to EN1993-1-3 for cross-section resistance and comparison between numerical and analytical results. Only models with *b*-parameter = 3 are presented here.

The ultimate resistance of cross-section from the finite element analysis showed a good agreement with EN-1993 part 1-3. However, some numerical models have a disagreement and show unsafe predictions compared to the design standard. Cluster of models with global slenderness $\bar{\lambda}$ = 1,25 and bolt spacing *b* = 3 and *b* = *4* exhibit considerably lower resistance than the design standard. Examination showed that these models are all models failed in interaction mode, i.e. distortional-flexural interaction. Therefore, it can be concluded that the analytical calculation based on EC1993-1-3 performed in this section corresponds to the numerical analysis carried out beforehand; whereas the deviations due to the interaction mode cannot be captured by EN 1993-1-3.

Table 5 Analytical calculation result of (a) the cross-section resistance and (b) buckling resistance for the studied columns according to EN1993-1-3 and comparison of the resistance to the FE results

(a) *b*-parameter=3

Model ID	d	t	λ	s/d	Class	Area	Cross section resistance						FE analysis	FE/ EC3-1-3
							Local	Eff. area local	Dist. slend	Dist.	Eff. area dist.	$N_{c,Rd}$		
						A_g	ρ_b	$A_{eff,loc}$	λ_d	χ_{dist}	$A_{eff,dis}$			
	[mm]	[mm]	[-]	[-]	[-]	[cm²]	[-]	[cm²]	[-]	[-]	[cm²]	[kN]	[kN]	[-]
1 2 3 1 3	500	9			3	157.0	1.0	157.0	0.79	0.898	141.0	5003.9	5625.7	1.12
1 3 3 1 3	700	12			3	293.5	1.0	293.5	0.81	0.882	258.9	9192.4	10583.1	1.15
1 4 3 1 3	900	15	0.65		3	472.0	1.0	472.0	0.82	0.874	412.8	14653.3	16670.0	1.14
1 2 5 1 3	500	7			3	123.0	1.0	123.0	0.85	0.853	104.9	3724.3	4132.5	1.11
1 3 5 1 3	700	10			3	245.8	1.0	245.8	0.86	0.851	209.2	7425.1	8309.6	1.12
1 4 5 1 3	900	13			3	410.7	1.0	410.7	0.86	0.850	349.3	12398.7	13828.6	1.12
1 2 3 2 3	500	9			3	157.0	1.0	157.0	0.81	0.884	138.8	4927.1	4865.7	0.99
1 3 3 2 3	700	12			3	293.5	1.0	293.5	0.83	0.868	254.6	9038.6	8974.8	0.99
1 4 3 2 3	900	15	1	3	3	472.0	1.0	472.0	0.85	0.859	405.4	14391.9	14330.1	1.00
1 2 5 2 3	500	7			3	123.0	1.0	123.0	0.88	0.836	102.8	3650.2	3665.2	1.00
1 3 5 2 3	700	10			3	245.8	1.0	245.8	0.88	0.827	203.2	7213.2	7105.3	0.99
1 4 5 2 3	900	13			3	410.7	1.0	410.7	0.88	0.833	342.2	12148.3	12124.6	1.00
1 2 3 3 3	500	9			3	157.0	1.0	157.0	1.28	0.542	85.1	3020.0	3335.7	1.10
1 3 3 3 3	700	12			3	293.5	1.0	293.5	1.29	0.540	158.6	5628.8	6192.9	1.10
1 4 3 3 3	900	15	1.25		3	472.0	1.0	472.0	1.29	0.539	254.2	9024.0	9958.4	1.10
1 2 5 3 3	500	7			3	123.0	1.0	123.0	1.28	0.543	66.7	2369.0	2606.7	1.10
1 3 5 3 3	700	10			3	245.8	1.0	245.8	1.29	0.540	132.7	4710.1	5177.7	1.10
1 4 5 3 3	900	13			3	410.7	1.0	410.7	1.29	0.538	221.0	7846.1	8656.9	1.10

(a) *b*-parameter=3

Model ID	d	t	λ	s/d	Class	Area	Buckling resistance					FE analysis	FE/ EC3-1-3
							Eff. Area	Flex.	Tor.	Flex-Tor	$N_{b,Rd}$		
						A_g	A_{eff}	χ_F	χ_T	χ_{FT}			
	[mm]	[mm]	[-]	[-]	[-]	[cm²]	[cm²]	[-]	[-]	[-]	[kN]	[kN]	[-]
1 2 3 1 3	500	9			3	157.0	141.0	0.819	1.0	0.819	4097.5	5625.7	1.37
1 3 3 1 3	700	12			3	293.5	258.9	0.820	1.0	0.820	7536.4	10583.1	1.40
1 4 3 1 3	900	15	0.65		3	472.0	412.8	0.820	1.0	0.820	12022.1	16670.0	1.39
1 2 5 1 3	500	7			3	123.0	104.9	0.824	1.0	0.824	3069.7	4132.5	1.35
1 3 5 1 3	700	10			3	245.8	209.2	0.824	1.0	0.824	6116.7	8309.6	1.36
1 4 5 1 3	900	13			3	410.7	349.3	0.824	1.0	0.824	10210.9	13828.6	1.35
1 2 3 2 3	500	9			3	157.0	138.8	0.611	1.0	0.611	3011.8	4865.7	1.62
1 3 3 2 3	700	12			3	293.5	254.6	0.613	1.0	0.613	5541.8	8974.8	1.62
1 4 3 2 3	900	15	1	3	3	472.0	405.4	0.614	1.0	0.614	8839.9	14330.1	1.62
1 2 5 2 3	500	7			3	123.0	102.8	0.621	1.0	0.621	2268.5	3665.2	1.62
1 3 5 2 3	700	10			3	245.8	203.2	0.621	1.0	0.621	4476.4	7105.3	1.59
1 4 5 2 3	900	13			3	410.7	342.2	0.620	1.0	0.620	7533.4	12124.6	1.61
1 2 3 3 3	500	9			3	157.0	85.1	0.466	1.0	0.466	1408.2	3335.7	2.37
1 3 3 3 3	700	12			3	293.5	158.6	0.468	1.0	0.468	2635.6	6192.9	2.35
1 4 3 3 3	900	15	1.25		3	472.0	254.2	0.469	1.0	0.469	4235.6	9958.4	2.35
1 2 5 3 3	500	7			3	123.0	66.7	0.477	1.0	0.477	1129.9	2606.7	2.31
1 3 5 3 3	700	10			3	245.8	132.7	0.476	1.0	0.476	2242.1	5177.7	2.31
1 4 5 3 3	900	13			3	410.7	221.0	0.476	1.0	0.476	3731.1	8656.9	2.32

5. CONCLUSION

Based on the results presented in this paper, the following conclusions can be drawn:

(1) For the proposed semi-closed built-up columns, there is no expression in the Eurocode for predicting the elastic critical buckling, either for sectorial or global buckling modes. FE analyses need to be performed to obtain accurate buckling and failure mechanism.

(2) From non-linear post-buckling analysis considering material, geometrical non-linearity and initial imperfections, it can be concluded that FE models in the range of the predefined parameters failed in predominant distortional mode. Models with high global slenderness, i.e. $\bar{\lambda}$ = 1.25, experienced distortional-flexural interaction with significantly lower resistance than the one failed in pure distortional mode. From this analysis it is suggested that for the models in this parametric study, distortional buckling may control the failure mechanism even when the elastic distortional buckling stress (f_{crd}) is higher than the elastic flexural buckling stress (f_{crf}). Moreover, it was noticed that members with high distortional and global slenderness have higher parameter sensitivity on the ultimate strength and failure mode interaction.

(3) Evaluation of ultimate resistance according to EN1993-1-3 shows that for members with $\bar{\lambda}$ = 0.65 and $\bar{\lambda}$ = 1.0 a good agreement was obtained, while for very slender columns $\bar{\lambda}$ = 1.25 a large scatter numerical results were in found in unsafe region. This corresponds to the FE results which exhibit a distortional-flexural interaction mode in those models. Therefore, it can be suggested that the expression (Eq. 5.12) used in EN1993-1-3 for reduction factor due to distortional buckling may be adopted for the semi-closed polygonal type of cross-section undergoes pure distortional buckling mode used in this parametric study, with provision of global slenderness, $\bar{\lambda}$ < 1.25. The EN1993-1-3 became the lower bound for the results of numerical ultimate strength. It is important to note that for this type of cross-section, a careful application of design standard shall be done since current design methods ignore buckling interaction and do not explicitly consider sectional buckling. Knowing the exact failure mode is necessary, in order to avoid too conservative predictions.

REFERENCES

Dubina, V. U. D. (2014). Erosion of Interactive Buckling Load of Thin-Walled Steel Bar Members: Contribution of. *Timisoara School"," Romanian Journal of Technical Sciences− Appl. Mechanics, 59*, 9-137.

European Comission. (2016). AEOLUS4FUTURE. Retrieved from http://www.aeolus4future.eu/about

European committee for standardization. (2006). *Eurocode 3: design of steel structures, part 1-3: General rules for cold formed thin gauge members and sheeting*. Retrieved from Brussels, Belgium: https://www.phd.eng.br/wp-content/uploads/2015/12/en.1993.1.3.2006.pdf

Garzon, O. (2013). *Resistance of polygonal cross-sections: application on steel towers for wind turbines.* Luleå tekniska universitet,

Hancock, G. (1997). Design for distortional buckling of flexural members. *Thin-walled structures, 27*(1), 3-12.

Heistermann, C. (2011). *Behaviour of pretensioned bolts in friction connections: towards the use of higher strength steels in wind towers.* Luleå tekniska universitet,

Moen, C. D. (2008). *Direct Strength Design for Cold-Formed Steel Members with Perforations.* The Johns Hopkins University, Baltimore. Retrieved from https://www.ce.jhu.edu/bschafer/dsm_holes/DSM_holes_AISI_draft%20R1.pdf

Ryan, B. (2017). *Finite Element Modelling and Parametric Studies of Semi-closed Thin-walled Steel Polygonal Columns – Application on Steel Lattice Towers for Wind Turbines.* (Master), Luleå University of Technology,

Schafer, B., & Peköz, T. (1999). *Local and distortional buckling of cold-formed steel members with edge stiffened flanges.* Paper presented at the Proceedings of the 4th International conference Light-weight steel and aluminium structures (ICSAS'99). Espoo, Finland.

Schafer, B. W. (2006). *Distortional buckling of cold–formed steel column, RESEARCH REPORT RP00-1* Retrieved from https://www.buildusingsteel.org/aisi-design-resources/-/media/doc/buildusingsteel/research-reports/CFSD%20-%20Report%20-%20RP00-1.pdf

Simulia, D. S. (2007). Abaqus/CAE user's manual. *Providence, RI, 2007*.

Teng, J.-G., & Rotter, J. M. (2006). *Buckling of thin metal shells*: CRC Press.

Veljkovic, M., Heistermann, C., Husson, W., Limam, M., Feldmann, M., Naumes, J., . . . Fruhner, K. (2012). *High-strength tower in steel for wind turbines (HISTWIN)*: European Commission Joint Research Centre.

Veljkovic, M., Heistermann, C., Tran, A., Feldmann, M., Möller, F., Richter, C., . . . Matos Silva, A. (2014). High steel tubular towers for wind turbines (HISTWIN2). *Brussels, Belgium*.

Yu, W.-W., LaBoube, R. A., & Chen, H. (2019). *Cold-formed steel design*: John Wiley & Sons.